Eur. Phys. J. B **8**, 293–300 (1999)

THE EUROPEAN PHYSICAL JOURNAL B
EDP Sciences

Weak localization and interaction in doped CdTe

W. Poirier[1], M. Sanquer[2,a], and K. Saminadayar[3]

[1] CEA-DSM-DRECAM-SPEC, CE Saclay, 91191 Gif sur Yvette Cedex, France
[2] CEA-DSM-DRFMC-SPSMS, CEA Grenoble, 38054 Grenoble Cedex 9, France
[3] CEA-DSM-DRFMC-SPMM, CEA Grenoble, 38054 Grenoble Cedex 9, France

Received 6 May 1998 and Received in final form 20 October 1998

Abstract. We study weak localization and electron interaction in CdTe:In by low temperature magnetoconductance experiments to quantify the phase breaking length and the importance of interactions in CdTe. Then we study superconducting contacts to CdTe:In by transport measurements at very low temperature. The conductance-voltage characteristics of the superconducting contact exhibits the main features of a SIN junction, with a superimposed zero bias anomaly. This anomaly in the density of states of CdTe is very sensitive to magnetic field and probably induced by the proximity of the superconducting contact.

PACS. 72.15.Rn Quantum localization – 72.80.Ey III-V and II-VI semiconductors – 74.50.+r Proximity effects, weak links, tunneling phenomena, and Josephson effects

The combined effect of disorder and interaction is probably responsible for an anomalous conducting phase in 2D films of high mobility semiconductors [1]. Both the mobility and the effective mass of carriers are important parameters which control the occurrence of the strong decrease of the film-resistance below typically one kelvin. The transition is not observed for electrons in GaAs (low effective electron mass $m^* = 0.067$) but exists for holes ($m^* = 0.3$) or for silicon MOSFETs of comparable mobility ($m^* = 0.4$). CdTe:In is an interesting case because its effective electron mass ($m^* = 0.11$) is intermediate between those of GaAs and Silicon. Heterostructures and 2D gases can be also realized [2].

For these reasons we present weak localization and electron-electron interaction studies in 3D, low mobility, CdTe:In samples. We show that the phase breaking time is relatively large at very low temperature, comparable to what is observed in GaAs:Si or metallic films ($\tau_\phi \simeq 2.5 \times 10^{-9}$ s below $T = 100$ mK). The temperature dependence of the conductance at very low temperature allows us to estimate the screening length and more generally the correction to conductivity due to interaction.

We have also studied CdTe:In/In contacts below the critical superconducting temperature of indium. Semiconductor-Superconductor (Sm-Su) contacts have been extensively studied in recent years, in relation with new mesoscopic proximity effects [4–6]. Most studies are devoted to GaAs, InGaAs or InAs-based structures. CdTe is an interesting material for studying Sm-Su contacts because ohmic contacts are obtained by deposition of indium films whereas Schottky contacts are observed with gold films. Thanks to this property, it is possible in principle to design geometries where a Schottky gate is placed very close to a superconducting contact, which is crucial for studying mesoscopic aspects of the Andreev reflection.

We will show that the sharp G(V) characteristics of In/CdTe:In contacts is of Superconductor-Insulator-Metal type (SIN). The transparency of the interface is small and we estimate the depairing rate for Cooper pairs near the interface. Nevertheless this material is promising for studying mesoscopic Andreev reflection. In particular we report the existence of a zero bias anomaly which is very sensitive to the magnetic field. By comparison with what we know from magnetoconductance experiments in the CdTe film, we can show that this anomaly is not directly related to electron interaction correction to the density of states in CdTe, but is induced by the proximity of the superconducting contact.

1 Weak localization and interaction corrections

The sample consists of a 2.7 μm thick nominally doped at 5×10^{23} In m^{-3} CdTe layer grown on a CdZnTe (0.04 Zn) substrate by molecular beam epitaxy [3]. The sample is chemically etched to form a Hall bar. The contacts are as-grown Indium films on the top of the CdTe crystal.

The Hall measurement shows that between $T = 30$ mK and $T = 4.2$ K, the carrier concentration is constant and equal to $n = 1.7 \times 10^{23}$ m^{-3}. We deduce $k_F = (3\pi^2 n)^{1/3} = 1.71 \times 10^8$ m^{-1}. The diffusion coefficient is calculated at $T = 4.2$ K to be $D \simeq 4 \times 10^{-4}$ m^{2}s^{-1}, that places the

[a] e-mail: msanquer@cea.fr ou sanquer@drfmc.ceng.cea.fr

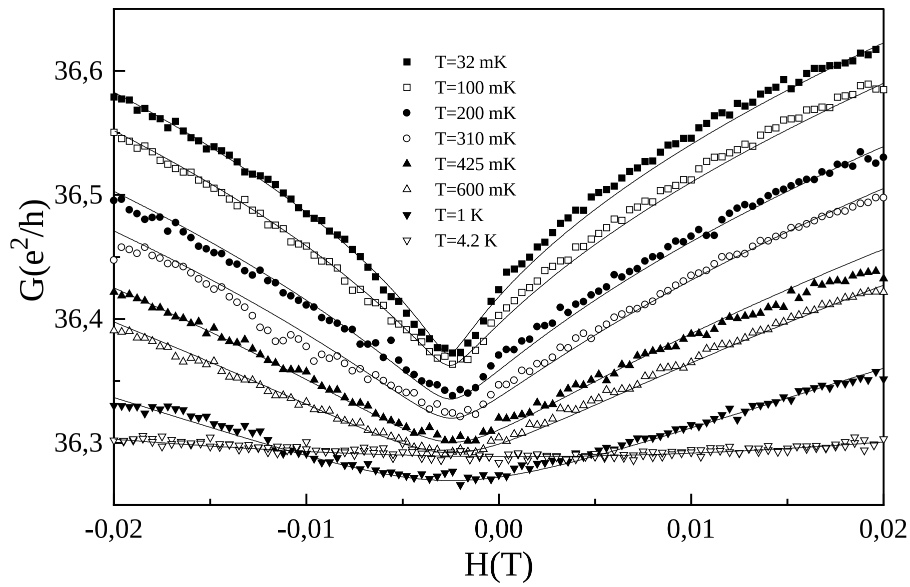

Fig. 1. Low field magnetoconductance of the CdTe film (3.33 squares in series) at various low temperatures. The solid lines are fits by the weak localization formula 2. Note that the conductance increases at low temperature.

sample very close to the Ioffe-Regel criterium $k_F\ell \simeq \pi$ for the Metal-Insulator transition. Following the Mott criterium, $n_c^{1/3}a_B \simeq 0.25$ [7], the metal-insulator transition (MIT) is expected to take place at a doping concentration of $1.25\times10^{23}\,\mathrm{e.m}^{-3}$ (the Bohr radius is $a_B = 5\,\mathrm{nm}$). Other characteristics of the sample are listed below: the resistance per square is 213 ohm. Between the voltage probes, the sample consists of 3.33 squares in series. The mobility is $\mu = 638\,\mathrm{cm^2V^{-1}s^{-1}}$ ($T = 4.2\,\mathrm{K}$).

The magnetoconductance (magnetic field perpendicular to the film and to the current) is plotted for different temperatures between $T = 30\,\mathrm{mK}$ and $T = 4.2\,\mathrm{K}$ in Figure 1. The low field magnetoconductance is typical for weak localization suppression by time reversal symmetry breaking in the absence of spin-orbit scattering. Because the sample is 3D (all dimensions are larger than the phase breaking length $L_\phi = \sqrt{D\tau_\phi}$, where τ_ϕ is the phase breaking time), the correction due to weak localization is given by (in the absence of any spin relaxation) [8]:

$$\Delta\sigma_{WL}(T) = \frac{1}{4}\frac{e^2}{2\pi^2\hbar}\left(\frac{1}{\ell} - \frac{1}{L_{\phi(T)}}\right) \qquad (1)$$

where the factor 1/4 is introduced in our weak localization fit (see later).

The positive magnetoconductance is given by:

$$\Delta\sigma(H) = \frac{1}{4}\frac{e^2}{2\pi^2\hbar L_H} f_3\left(2\frac{L_\phi^2}{L_H^2}\right) \qquad (2)$$

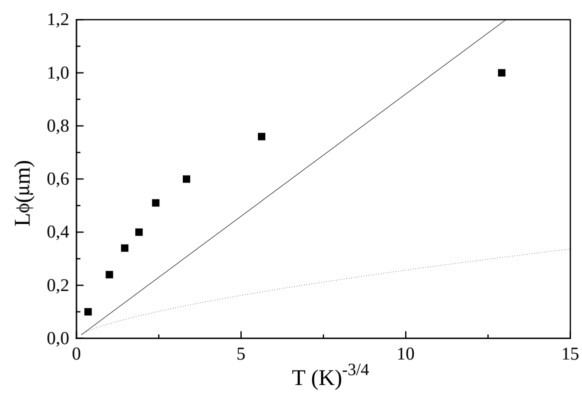

Fig. 2. The phase breaking length estimated from the localization fit in Figure 1, *versus* temperature. The solid line is the estimation by equation (4). The dotted line is the estimation for the thermal length.

with

$$f_3(x) = \sum_{n=0}^{\infty}\left(2\left(\sqrt{n+1+\frac{1}{x}} - \sqrt{n+\frac{1}{x}}\right) - \frac{1}{\sqrt{n+\frac{1}{x}+\frac{1}{2}}}\right) \qquad (3)$$

(the expression $f_3(x)$ is roughly equal to $x^{3/2}/48$ if $x \ll 1$ and $f_3(x) \simeq 0.605$ if $x \gg 1$). The magnetic length is $L_H = \sqrt{\frac{\hbar c}{2\,eH}}$. The solid lines in Figure 1 are the fits by equation (2). The prefactor 1/4 is our phenomenological parameter. Such a prefactor could be due to the proximity of the metal-insulator transition. It does not affect the magnetic field dependence of the conductance which gives

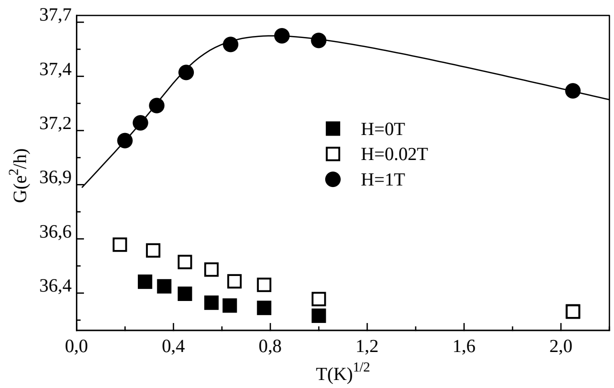

Fig. 3. Conductance of the CdTe film (3.33 squares in series) as a function of temperature for three magnetic fields. The solid line is the fit by equation (7) for $H = 1$ T. The maximum of conductance occurs when the Zeeman splitting is approximately equal to the thermal energy.

the value of L_ϕ. Figure 2 shows the variation of the phase breaking length with temperature. We obtain $L_\phi \simeq 1\,\mu$m at $T = 30\,$mK. It corresponds to a relatively large phase breaking time of $25\times10^{-10}\,$s, comparable to or larger than the values observed in GaAs:Si samples or metallic films. If electron-electron scattering is the dominant energy relaxation process, Altshuler *et al.* [8] obtain:

$$\frac{1}{\tau_\phi} = \frac{2e^2}{\pi^2\hbar\sigma\sqrt{2D}}\left(\frac{k_bT}{\hbar}\right)^{3/2} \quad (4)$$

where $\sigma = \frac{1}{R_{square}W}$ is the conductivity and W the thickness. This gives $\frac{1}{L_\phi} \propto T^{3/4}$ and $L_\phi \simeq 92\,$nm at $T = 1\,$K ($\tau_\phi \simeq 2.1\times10^{-11}\,$s). The prediction of equation (4) is plotted as a solid line in Figure 2. It gives the right order of magnitude for the phase breaking time, but not the right evolution, which follows the $\frac{1}{L_\phi} \propto T^{3/4}$ dependence at high temperature with a prefactor approximately 2.5 times larger in the experiment, and shows a saturation at low temperature. The observation of the saturation is a common fact (see for instance [14]), and the prefactor could be eventually due to an underestimation of the diffusion constant D, due to uncertainties in the effective thickness of the film. Another explanation for the pseudo-saturation of L_ϕ could be a dimensionality crossover between $L_\phi \ll W$ at high temperature (3D) and $L_\phi \simeq W$ at low temperature (2D) ($W = 2.7\,\mu$m is the nominal thickness of the doping). In the 2D case, the predicted temperature dependence is $L_\phi \propto T^{1/2}$, weaker than in the 3D case. Nevertheless our largest L_ϕ is still smaller than W. Our estimation of L_ϕ is typically ten times smaller than the one obtained in CdTe:In doped at $\simeq 10^{24}\,\mathrm{m}^{-3}$ in reference [9]. This is not surprising because at this concentration the sample is more in the metallic regime and the diffusion constant is larger.

An interesting point is that, at very low temperature the conductance of the sample increases as the temperature is lowered (at low magnetic field) (see Fig. 1), suggesting that a positive increasing electron-electron interaction (EEI) correction overcomes the weak localization correction itself. In the opposite case the conductance should decrease when the weak localization grows as the temperature decreases. The situation is similar to the case of 3D Si:P for doping concentration typically twice the critical concentration for the MIT [10–12]. The electron interaction correction overcomes the weak localization correction if the thermal length $L_T = \sqrt{\frac{\hbar D}{k_BT}}$ is much smaller than the phase breaking length, which is realized in our sample ($L_T \simeq 55\,$nm at $T = 1\,$K). In fact the EEI correction is given by [8]:

$$\Delta\sigma_{EEI}(T) = 0.915\frac{e^2}{2\pi^2\hbar}\left(\frac{2}{3}+\frac{3\lambda^{(j=1)}}{4}\right)\left(\frac{1}{\ell}-\frac{1}{L_T}\right). \quad (5)$$

The first universal term describes interaction between an electron and a hole with parallel spins and is due to the exchange (Fock) term while $\lambda^{(j=1)}$ is related to the direct (Hartree) term in the Hartree-Fock approximation of the Coulomb repulsion ($\lambda^{(j=1)}$ is negative). In the absence of any attractive virtual potential between electrons, $\lambda^{(j=1)}$ depends only on the Fermi surface and on the screening length. The exchange term dominates the Hartree term, if the interaction potential is sufficiently smooth, *i.e.* its extension is larger than λ_F. A positive EEI correction $((\frac{2}{3}+\frac{3\lambda^{(j=1)}}{4}) \leq 0)$ means on the contrary that the Hartree part is dominant over the exchange part in the correction (Eq. (5)).

For magnetic fields higher than $H_c = \frac{k_bT}{g\mu_B}$, the spin degeneresence is broken by Zeeman splitting, and the correction due to interaction becomes [8]:

$$\Delta\sigma_{EEI}(T) = 0.915\frac{e^2}{2\pi^2\hbar}\left(\frac{2}{3}+\frac{\lambda^{(j=1)}}{4}\right)\left(\frac{1}{\ell}-\frac{1}{L_T}\right). \quad (6)$$

The Zeeman splitting reduces the Hartree contribution by a factor of three. The exchange contribution, which is insensitive to the Zeeman effect because it concerns electrons and holes with parallel spins, becomes dominant with respect to the Hartree term. The temperature dependence for the conductance is then reversed as seen in Figure 3 for a magnetic field of 1 T.

More precisely, the temperature dependence at $H = 1\,$T could be fitted over all the temperature range with the following equation, whose limits for $k_bT \leq g\mu_BH$ and $k_bT \geq g\mu_BH$ are respectively equations (5, 6) [8]:

$$\Delta\sigma_{EEI}(T,H) = \frac{e^2}{2\pi^2\hbar}\left(\frac{2}{3}+\frac{\lambda^{(j=1)}}{4}\left(3-2f_3\left(\frac{g\mu_bH}{k_BT}\right)\right)\right) \times\left(\frac{1}{\ell}-\frac{1}{L_T}\right) \quad (7)$$

where $f_3(x) = \int_0^\infty d\omega\frac{\delta^2}{\delta^2\omega}(\omega N(\omega))(\sqrt{\omega+x}+\sqrt{|\omega-x|}-2\sqrt{\omega})$ and $N(\omega) = \frac{1}{\exp(\omega)-1}$.

Two parameters enter essentially in the fit: the Landé factor g and $\lambda^{(j=1)}$. $\lambda^{(j=1)}$ depends only on the Fermi surface and on the screening length; in three dimensions

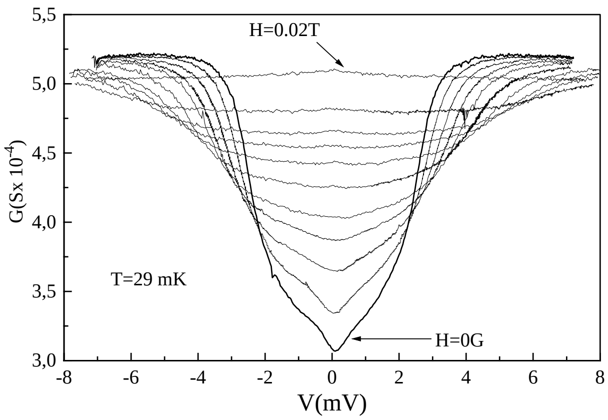

Fig. 4. Conductance of the semiconducting film (7.7 squares in series) and the two superconducting Indium junctions *versus* voltage at various magnetic fields from 0 to 0.02 T (values of field are respectively: 0, 35, 40, 45, 50, 60, 70, 80, 89, 110 and 200 $\times 10^{-4}$ T). The temperature is $T = 29$ mK.

(if there is no electron-electron interaction *via* virtual phonon exchange) [8]:

$$\lambda^{(j=1)} = \frac{32}{3}\,\frac{1+3/4F-(1+F/2)^{3/2}}{F} \tag{8}$$

and

$$F = \frac{2}{x^2}\ln(1+x^2) \tag{9}$$

with $x = \frac{2k_F}{k_{screening}}$.

The solid line in Figure 3 ($H = 1$ T) is obtained with $|g| \simeq 0.6$ and $\lambda^{(j=1)} \simeq -1.03$, equivalent to $F \simeq 1.12$. This corresponds to $k_{screening} \simeq 2.48 \times 10^8\,\mathrm{m}^{-1}$.

$k_{screening}$ is close to the calculated screening wave vector in the Thomas-Fermi approximation (ϵ_r is 10.5 in CdTe):

$$k_{TF} = \left(\frac{k_F m^* e^2}{\pi^2 \epsilon_r \epsilon_0 \hbar^2}\right) \simeq 2.07 \times 10^8\,\mathrm{m}^{-1} \tag{10}$$

We have been forced to multiply the theoretical values for $\Delta\sigma_{EEI}$ by a constant factor of 0.7, whose origin is not explained. This factor does not affect the determination for $\lambda^{(j=1)}$. Note that the change of sign for the correction occurs as $T \simeq \frac{g\mu_B H}{k_B} \simeq 0.4\,\mathrm{K}$ (for $|g| \simeq 0.6$): for higher temperatures, the Zeeman splitting is not resolved and the correction is proportional to $(\frac{2}{3} + \frac{3\lambda^{(j=1)}}{4})$, and for lower temperatures the correction is proportional to $(\frac{2}{3} + \frac{\lambda^{(j=1)}}{4})$. The fitted Landé factor is comparable to its theoretical estimation ($g = -0.62$), but lower than observed by electron paramagnetic resonance experiments ($g = -1.7$) [13]. $g = -1.7$ would produce a change of sign for the conductance correction for $H = 1$ T at $T \simeq 1.14\,\mathrm{K}$. In Figure 3, no change is seen for $T^{0.5} = (1.14)^{0.5} \simeq 1.07$.

Summing the corrections due to interaction and weak localization, the temperature dependence of the conductivity at zero magnetic field is given by ($T_2 \leq T_1$):

$$\sigma(T_2) - \sigma(T_1) = \frac{e^2}{2\pi^2\hbar}\left(\frac{1}{4}(L_\phi^{-1}(T_1) - L_\phi^{-1}(T_2))\right) + 0.915 \times 0.7\left(\frac{2}{3} + \frac{3\lambda^{(j=1)}}{4}\right)(L_{T_1}^{-1} - L_{T_2}^{-1}) \tag{11}$$

(the factors 1/4 and 0.7 are the phenomenological parameters introduced in our fits for the low field magnetoconductance and for the temperature dependence at $H = 1$ T)

Equation (11) includes too many parameters for a real adjustment. Nevertheless the variation of conductivity between our lowest temperature (35 mK) and 1 kelvin for instance is in agreement with equation (11): at $T = 35\,\mathrm{mK}$ (resp. 1 K), $L_\phi \simeq 1\,\mu\mathrm{m}$ and $L_T \simeq 0.3\,\mu\mathrm{m}$ (resp. $L_\phi \simeq 0.25\,\mu\mathrm{m}$ and $L_T \simeq 0.055\,\mu\mathrm{m}$). For zero field we calculate $\Delta\sigma \simeq -3.2\,\Omega^{-1}\mathrm{m}^{-1}$ in rather good agreement with the observed $\Delta\sigma \simeq -5.2\,\Omega^{-1}\mathrm{m}^{-1}$ (or $\Delta G \simeq 0.1 = \frac{1}{3.333}\Delta\sigma W \frac{e^2}{h}$ in quantum units, see Fig. 3), if one considers that $\Delta\sigma$ results from the *difference* of two large opposite terms, the weak localization and the interaction correction.

At $H = 200 \times 10^{-4}\,\mathrm{T}$, the weak localization contribution in equation (11) is strongly reduced, and the Zeeman splitting is still not resolved. We calculate $\Delta\sigma \simeq -12.4\,\Omega^{-1}\mathrm{m}^{-1}$ and we measure $\Delta\sigma \simeq -12.5\,\Omega^{-1}\mathrm{m}^{-1}$ (or $\Delta G \simeq 0.265 = \frac{1}{3.333}\Delta\sigma W \frac{e^2}{h}$ in quantum units, see Fig. 3).

In conclusion of this section, we have found that our CdTe:In film is close to the metal-insulator transition, but that the phase breaking time is relatively large and the screening of the Coulomb repulsion is strong. We obtain a reasonable agreement with the theories of both weak localization and interaction correction in the diffusive regime [8]. This considerations are very important in the context of the mesoscopic proximity effect near superconducting contacts, because the phase breaking length fixes the scale for the mesoscopic effects, and interactions in the normal metal (or doped semiconductor) affect strongly the proximity effect. We now consider contacts to superconducting Indium films.

2 Superconducting contacts

Figure 4 shows the G-V characteristics of two In-CdTe contacts in series with approximately 7.7 squares of the CdTe film at the lowest temperature, for various magnetic fields. The two $380\,\mu\mathrm{m}^2$ diameter circular superconducting contacts are directly on the top of the CdTe:In layer (a Hall bar of width $300\,\mu\mathrm{m}$ is defined by etching; the separation between the centers of the indium contacts is $2400\,\mu\mathrm{m}$). The contact are as-grown without any surface or annealing treatments.

For zero magnetic field the G-V curve shows a pronounced dip for bias below 2 mV. This value is larger than twice the superconducting gap of the Indium contact, which is evaluated to be $650\,\mu\mathrm{eV}$, because of the

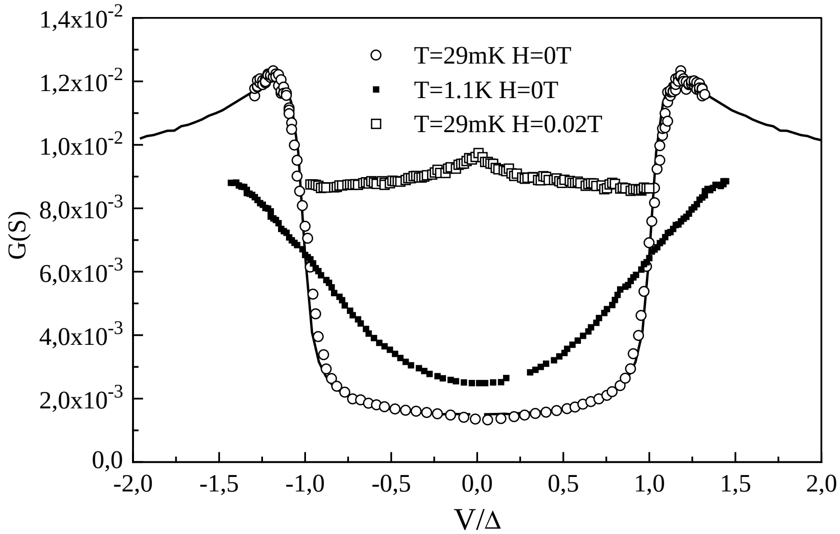

Fig. 5. The deduced conductance for each CdTe/Indium contact *versus* the voltage normalized to the Indium superconducting gap $\Delta \simeq 650\,\mu$V. The solid line is the BTK fit, in a planar geometry (see the text). The open circles are in zero magnetic field at the lowest temperature, the open squares for the lowest temperature at $H = 0.02$ T and the solid squares for zero field and $T = 1.1$ K.

voltage drop across the semiconducting film. Above this bias the conductance is slightly enhanced as compared to its normal state value, obtained above the indium critical superconducting temperature, or at high magnetic field. An extra dip in conductance near zero voltage appears at small magnetic field.

Figure 4 shows the raw data and it is necessary to take into account the resistance of the CdTe film between the two superconducting contacts (1655 ohms) to obtain the G-V characteristics of each Su-Sm contact. The data in Figures 5 and 6 are obtained after this (simple) numerical treatment. Figure 5 shows the conductance *versus* bias for *each superconducting contact* at the lowest temperature for zero magnetic field and for $H = 2 \times 10^{-2}$ T, and at $T = 1.1\,$K for $H = 0$ T. The bias is calculated across each contact and normalized to the estimated value for the indium critical voltage ($\Delta \simeq 650\,\mu$eV).

The large absolute value of the contact resistance corresponds to a small transparency per channel at the interface. In a planar junction, the current is injected through the whole surface of the contact and then is forced to flow transversally through the thickness of the CdTe:In layer. The resistance per square of the normal semiconducting film is relatively large, and it is easy to show by simple resistance network calculations that the extension of the current lines under overlap is given by $\mathcal{L} \simeq \sqrt{R_b/R_N}$ (R_N is the resistance per square of the semiconductor and R_b is the specific resistance of the barrier). The total normal resistance of each junction (planar NS interface + Semiconductor under the junction) is given by $R_{Tot} \simeq \sqrt{R_b R_{square}/\mathcal{W}}$ (for $\mathcal{L}$ smaller than the overlap, $\mathcal{W}$ denotes the transverse length of the overlap border). *Neglecting all interference phenomena due to the confinement in the planar junction*, we are able to estimate the value of the normal specific junction resistivity: $R_b \simeq 5.0 \times 10^{-2}\,\Omega\mathrm{cm}^2$, and to fit all the G-V characteristics [16]. The estimation for the barrier transmission t should be consistent with the absolute measured value of the normal contact resistance, *via* the relation $t = \frac{h}{R_b 2e^2}(\frac{2}{\lambda_F})^{-2}$. Supposing the barrier is homogeneous, the latter relation implies a very small t (4×10^{-7}).

In that case one can neglect Andreev reflection processes which are proportional to $t^2 \ll t \ll 1$ (two electrons could be transferred though the N-S interface to form a Cooper pair in the superconducting bank). So considering the interface in the tunneling approximation, the differential conductance is proportional to the densities of states near the junction both in indium and in CdTe. We have used the formalism of Blonder, Tinkham and Klapwijk (BTK) [15], adapted to the case of a planar junction with a highly resistive normal bank. Indeed the BTK theory considers a one-dimensional ballistic junction. But because the differential conductance depends strongly on the actual voltage and as the CdTe film is resistive, the conductance through the junction is not constant at different distances from the overlap border. The solid line in Figure 5 is our fit where we use the BTK formalism taking into account the variation in voltage across the junction due to the finite resistance of the semiconducting film under the superconducting contact overlap [16].

The fit includes the following parameters: the superconducting gap Δ, the temperature, the transmission of the barrier t and a depairing rate Γ, which could also represent a smoothing of the superconducting gap near the interface; In both cases the gap parameter Δ in the theory is formally replaced by $\Delta + i\Gamma$ [17,18].

The fit should first take into account the reduction in conductance at zero bias as compared to bias above the superconducting gap. The observed factor of 6 is large for a superconductor-semiconductor contact.

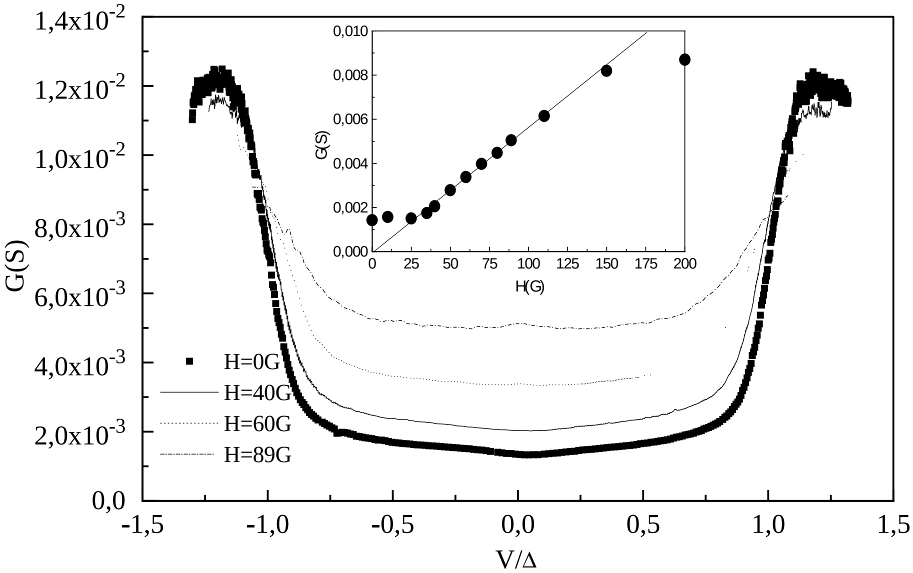

Fig. 6. The deduced conductance for each CdTe/Indium contact, normalized to the Indium superconducting gap $\Delta \simeq 650\,\mu$V, *versus* magnetic field. The inset shows the linear increase of zero bias conductance with magnetic field.

One can explain quantitatively this factor of 6 in three different ways: the transmission per channel t is about 1/6 and $G(V=0) \propto t^2 \simeq 1/6G(\text{eV} \gg \Delta) \propto t$; with this value, as said before, one attempts a unrealistic low specific contact resistance, except if the barrier is very inhomogeneous and the effective surface of conducting links is percentiles of the whole surface. In principle it is possible in that case to use the BTK formalism without Γ parameter (not done here). The second way is somewhat similar to the first one, because it supposes inhomogeneities; but one suppose that the contact resistance is large and homogeneous and that Indium is partially superconducting and partially normal. At small bias, the contact resistance is much lower in front of the normal regions (than of the superconducting ones) and provides an effective shunt for the current below the gap. This is what is happening in magnetic field (see later).

We have chosen to explain our results in a third way which is to introduce the depairing rate Γ which smoothes the BCS density of states in Indium. This depairing rate $\Gamma = 16\,\mu$V is small as compared to the superconducting gap $\Delta \simeq 650\,\mu$eV.

With this value the fit does not depend on the *small* value for t the transparency per channel (except for the absolute value of the tunnel conductance of course). We have chosen $t = 4\times10^{-7}$, but we know that fit is not changed if $t \ll 1/6$. Figure 5 shows the excellent agreement between our fit and the experimental data at low temperature. The advantage of this procedure with a depairing rate is to avoid the hypothesis of non uniform transmission through the contact, that is not really justified in our as-grown contacts.

Note that a small decrease of the conductance near zero bias is not properly fitted. We attribute this features to anomalies in the CdTe density of states near the contact, which are not included in the fit (see later).

The effect of a magnetic field $H = 2 \times 10^{-2}$ T is to destroy completely the dip in differential conductance seen at voltage below the gap. This field is comparable to the critical field for the superconductivity of bulk indium ($H = 2.9\times10^{-2}$ T). Figure 6 shows the evolution of G(V) for one CdTe/Indium junction at small fields. The inset shows a linear dependence of the linear conductance *versus* the magnetic field (between $H = 25\times10^{-4}$ T and $H = 150\times10^{-4}$ T). This dependence is understood if we suppose that a normal tunnel junction NIN conductance is added to the SIN conductance at zero field. This is what is expected, when the magnetic flux progressively penetrates the indium film.

In addition to the main features of the G-V curves and their evolution with magnetic field to a normal conductance, it is clear that the differential conductance exhibits anomalies near zero voltage. For $H = 200\times10^{-4}$ T, the superconductivity of indium is destroyed, and the G-V curves of junctions show a pronounced *increase* at low voltage. This is due to the *increase* of the density of states due to interaction in CdTe. Figure 7 shows the normalized variation of the conductance *versus* bias for the 2 probes measurement with Indium contacts ($H = 0.02$ T, the Indium is normal) as compared to the conductance variation for the CdTe film (4 probes measurement). The zero bias anomaly is partly due to the change in the CdTe film conductance and partly due to the anomaly in the In/CdTe contact conductance, which directly reflects the density of states in CdTe close to the junction. This is because the voltage drop is divided between the two contact resistances and the CdTe film. Nevertheless one sees that the relative conductance anomaly is more important on the tunnel resistance through the contacts than on the normal resistance of the film (if not, the relative effect would be the same or less in the 2-probes case). We note that the observation of a peak at zero bias in the tunneling

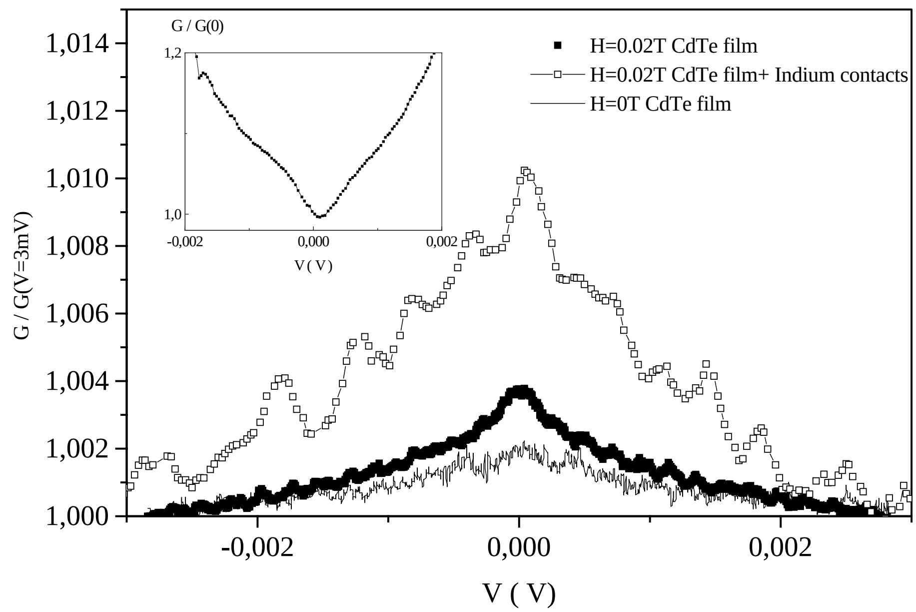

Fig. 7. Differential conductance (normalized to its value at $V = 3$ mV) *versus* voltage in the CdTe film (4 probes measurement) (solid squares: $H = 0.02$ T, line: $H = 0$ T) and in the CdTe film in series with two Indium contacts (2 probes measurement, open squares: $H = 0.02$ T; inset: $H = 0$ T). Note the larger variation of conductance due to the zero bias anomaly of the tunnel conductance through CdTe/In contacts (open squares) as compared to the zero bias anomaly in the CdTe film only (solid squares). Inset: differential conductance (normalized to its value at $V = 0$ V) *versus* voltage in the CdTe film in series with two Indium contacts (2 probes measurement). The conductance exhibits a dip at zero voltage instead of a peak (see the text).

conductance of superconductor/barrier/disordered metal is an exception (see [8] and references therein).

At zero magnetic field, instead of a peak in conductance at zero bias, the characteristics exhibits a *deficit* of conductance near zero bias (see Fig. 4 and the inset of Fig. 7). This deficit is rapidly destroyed by the magnetic field. This deficit is not due to the weak localization or interaction correction in the film, that increases the conductance at small energy (see Figs. 3, 7). Either, this dip is not due to the modification of the density of states by solely the screened Coulomb interaction in CdTe near the contact. As shown before this effect tends to increase the conductivity at low energy that reflects a peak in the density of states at the Fermi energy (see [8]). Consequently the dip is due to the presence of superconductivity in the indium electrode.

This dip could be due to an interference effect near the superconducting contact. Note in particular its sensitivity to an applied magnetic field: it is destroyed by a magnetic field of 50×10^{-4} T (see Fig. 4). Such sensitivity to magnetic field tends to exclude arguments in terms of Coulomb blockade near the tunnel junction [19].

It has been shown both theoretically [20] and experimentally [21] that the density of states in a normal metal in close contact with a superconductor is deeply modified by the proximity effect. A dip in the density of states appears at small energy (from the Fermi level) which is very sensitive to the magnetic flux: the effect is killed when the electron-hole symmetry is broken by the magnetic field ($H \geq \frac{h}{eL_T^2}$) or the voltage ($eV \geq \frac{\hbar D}{L_T^2}$). In the case where the SN contact transparency is low, the confinement in the normal metal near the interface could produce qualitatively the same effect [22]. It is very likely that mesoscopic proximity effect, occurring near an SIN junction, where N is a strongly disordered material, like CdTe near the MIT, is responsible for the conductance decrease near zero bias at zero magnetic field. A similar deep of conductance near zero bias at very low temperature and zero magnetic field has already been reported in GaAs/GaAlAs heterostructures contacted with Sn-Ti [23].

3 Conclusions

We have investigated interferences and interactions in CdTe:In films. The material is interesting for various aspects: the phase breaking time is long, the electron interactions are screened, in agreement with the Thomas-Fermi approximation, and finally the native contact with indium is not too resistive and shows sharp SIN characteristics as compared to other superconductor-semiconductor contacts. In addition a strong anomaly appears in the density of states of CdTe near the junction which could be attributed to the mesoscopic proximity effect, even if the contact resistance is large. These conclusions make the materials promising both in the context of mesoscopic superconductivity in superconducting-semiconducting junctions, and for the study of new anomalous conducting phases in two dimensional semiconductors with relatively large effective mass.

References

1. S.V. Kravchenko *et al.*, Phys. Rev. Lett. **77**, 4938 (1996); Physics Today July, 19 (1997).
2. K. Kheng, R.T. Cox, Y. Merle d'Aubigne, F. Bassani, K. Saminadayar, S. Tatarenko, Phys. Rev. Lett. **71**, 11 (1993); R.T. Cox, K. Kheng, K. Saminadayar, T. Baron, S. Tatarenko, in "High magnetic fields in the physics of semiconductors", edited by D. Heiman (World Scientific Pub. Co, 1995).
3. F. Bassani, S. Tatarenko, K. Saminadayar, N. Magnea, R.T. Cox, A. Tardot, J. Appl. Phys. **72**, 2927 (1992).
4. A. Kastalsky *et al.*, Phys. Rev. Lett. **67**, 3026 (1991).
5. B.J. Van Wees *et al.*, Phys. Rev. Lett. **69**, 511 (1992).
6. J.R. Gao *et al.*, Surface Science **305**, 470 (1994); H. Takayanagi, Physica B **218**, 113 (1996); H. Kroemer *et al.*, Physica B **203**, 298 (1994).
7. N.F. Mott, Phil. Mag. **6**, 287 (1961).
8. B.L. Altshuler, A.G. Aronov, *EEI in disordered systems*, edited by A.L. Efros, M. Pollack (North Holland, Amsterdam, 1985); B.L. Altshuler *et al.*, in *Physics Reviews*, edited by I.M. Khalatnikov (Harwood Academic Publishers, Switzerland, 1987), p. 225.
9. J. Jaroszynski *et al.*, Surface Science **361/362**, 718 (1996).
10. T.F. Rosenbaum *et al.*, Phys. Rev. Lett. **47**, 1758 (1981).
11. S. Bogdanovich *et al.*, Phys. Rev. Lett. **74**, 2543 (1995).
12. P. Dai *et al.*, Phys. Rev. B **45**, 3984 (1992).
13. K. Saminadayar, D. Galland, E. Molva, Solid State Comm. **49**, 627 (1984).
14. P. Mohanty *et al.*, Phys. Rev. Lett. **78**, 3366 (1997).
15. G.E. Blonder, M. Tinkham, T.M. Klapwijk, Phys. Rev. B **25**, 4515, 1982.
16. W. Poirier, Ph.D thesis, University of Paris 6 (1997). An interesting point is that $G(V=0)/G(\mathrm{eV} \gg \Delta) \propto \sqrt{t}$ in a planar geometry instead of $\propto t$, in the 1D BTK formalism.
17. Y. de Wilde *et al.*, Physica B **218**, 165 (1996) and references therein.
18. S.H. Tessmer *et al.*, Phys. Rev. Lett. **77**, 924 (1996).
19. A.N. Cleland, J.M. Schmidt, J. Clarke, Phys. Rev. Lett. **64**, 1565 (1984).
20. for a review see: C.W.J. Beenakker, Rev. Mod. Phys. **69**, 3 (1997).
21. H. Pothier *et al.*, Phys. Rev. Lett. **79**, 3490 (1997).
22. A.F. Volkov, A.V. Zaitsev, T.M. Klapwijk, Physica C **210**, 21 (1993).
23. K.M.H. Lenssen *et al.*, IEEE Trans. App. Superconductivity **3**, 1961 (1993); K.M.H. Lenssen *et al.*, Appl. Phys. Lett. **63**, 2079 (1993).